Article

Not peer-reviewed version

Adsorption of Pb2+ by Activated Carbon Produced by Microwave Assisted K2CO3 Activation of Leaf Sheath Fibre of Date Palm

Khaled D. Alotaibi *, Bassim H. Hameed , Hattan A. Alharbi , Saud S. Aloud , John P. Giesy

Posted Date: 6 September 2023

doi: 10.20944/preprints202309.0321.v1

Keywords: Activated carbon, metal ions, Phoenix dactylifera L., isotherm, kinetic, microwave irradiation, biochar

Article

Adsorption of Pb2+ by Activated Carbon Produced by Microwave Assisted K2CO3 Activation of Leaf Sheath Fibre of Date Palm

Khaled D. Alotaibi [1,*], Bassim H. Hameed [2], Hattan A. Alharbi [3], Saud S. Aloud [1] and John P. Giesy [4,5,6]

[1] Department of Soil Science, College of Food and Agriculture Sciences, King Saud University, P.O. Box 2460, Riyadh 11451, Saudi Arabia
[2] Department of Chemical Engineering, College of Engineering, Qatar University, P.O. Box 2713, Doha, Qatar
[3] Department of Plant Protection, College of Food and Agriculture Sciences, King Saud University, P.O. Box 2460, Riyadh 11451, Saudi Arabia
[4] Department of Veterinary Biomedical Sciences and Toxicology Centre, University of Saskatchewan, Saskatoon, SK S7N 5B3, Canada
[5] Department of Integrative Biology and Integrative Toxicology Program, Michigan State University, East Lansing, MI 48824, USA
[6] Department of Environmental Sciences, Baylor University, Waco, TX 76798, USA
* Correspondence: khalotaibi@ksu.edu.sa

Abstract: Date palm trees generate large amounts of various types of waste, including leaf sheath fibers which can be used as a low-cost, precursor for production of biochar including activated carbon (AC) that can be employed for adsorption of contaminants. In the current study, activated carbon was made from leaf sheath fibers of date palm (LSDPFAC) by use of chemical activation with K_2CO_3, combined with microwave irradiation, characterized and evaluated for its adsorptive capacity of lead ions (Pb^{2+}). The Brunauer–Emmett–Teller (BET) surface area, Langmuir surface area, total pore volume and average pore diameter of LSDPFAC were 560.20 m^2/g, 744.31 m^2/g, 0.29 cm^3/g and 2.47 nm respectively. When the initial concentrations of Pb^{2+} were increased from 1 to 10 mg/L, Pb^{2+} adsorption increased from 0.97 to 8.76 mg/g, dry mass (dm) while the percent of Pb^{2+} removed decreased from 96.70 to 87.60%. The greatest removal of Pb^{2+} occurred at pH 13 with adsorption capacity of 9.15 mg/g, dm. Results of isotherm and kinetic studies demonstrated that adsorption of Pb^{2+} onto LSDPFAC was best described by the Freundlich isotherm and pseudo-second order (PSO) models. Langmuir monolayer adsorption capacity, Q_m was 14.10 mg/g. Thermodynamic parameters of $\triangle H°$, $\triangle S°$, $\triangle G°$ and E_a were 6.39 kJ/mol, 0.12 kJ/mol.K, -31.28 kJ/mol and 15.90 kJ/mol, respectively, which demonstrated that adsorption of Pb^{2+} by LSDPFAC was endothermic, spontaneous and governed by physisorption.

Keywords: activated carbon; metal ions; *Phoenix dactylifera* L.; isotherm; kinetic; microwave irradiation; biochar

1. Introduction

Due to the existence of many pollutants in the water supplies, around the globe, more than 700 million people do not have access to drinkable water (Rajendran et al., 2022). Some of the most common water contaminants are metals, including lead (Pb), zinc (Zn), nickel (Ni), cadmium (Cd), chromium (Cr), copper (Cu), Arsenic (As) and mercury (Hg). Although all countries have fixed the maximum permissible concentrations of metals in surface waters, these rules are difficult to enforce under realistic situations (Liu et al., 2021c, Xiang et al., 2022). When present at concentrations that exceed permissible concentrations, these metals can cause adverse effects and impart serious health problems to humans, such as damaging kidney, nerve tissue and liver. Furthermore, they can be cancerous towards vital organs including bladder, skin and lung (Iqbal and Yahya, 2021, Yusop et al., 2022a, Mirzabeygi et al., 2017). Besides that, metals are able to cause various illness in bones,

muscles, fats and joints of people (Afroze and Sen, 2018). One of the most hazardous metals is lead (Pb^{2+}), which is released to the lithosphere during processes, including metallurgy mining, lead-acid battery factories, vehicle exhaust and tin-lead solder in domestic pipes (Zeng et al., 2017). Lead has been directly connected to severe diseases including pathology of the liver, malfunction of the kidney, rupture of central nervous system and infertility (Rezania et al., 2022, Goswami et al., 2017, Du et al., 2022). Moreover, Pb^{2+} is associated with diseases like encephalopathy and anaemia (Zhang et al., 2018). Due to these negative effects, treatment of Pb^{2+} has become an interest to many researchers around the globe.

There are a range of methods employed to remove Pb^{2+}, including ion exchange (Gupta et al., 2018), electro-chemical (Xu et al., 2018), electro-dialysis (Gherasim et al., 2014), membrane filtration (Azamat et al., 2021) and biological process (Lystvan et al., 2021). Furthermore, adsorption using activated carbon (AC) is another method that has been described as one of the best methods due to several key factors. First, this method is fast where equilibrium can be obtained in as little as 45 minutes (Manfrin et al., 2021). Second, adsorption is versatile in adsorbing a wide range of contaminants including metals (Yusop et al., 2022b, Kongsune et al., 2021), dyes (Azmier et al., 2021, Yusop et al., 2021a, Alharbi et al., 2022a), caffeine (Quesada et al., 2022), pesticide (Aziz et al., 2021), carbon dioxide (Li et al., 2022) and many more. Third, adsorption process is relatively easy and economically feasible since biochar can be derived from low-cost biomass wastes, such as corn fibre (Mbarki et al., 2022), orange peels (Ramutshatsha-Makhwedzha et al., 2022), teak wood (Firdaus et al., 2022), date palm bark wastes (Haghbin and Niknam Shahrak, 2021), acacia wood (Yusop et al., 2021b), mango seeds (Lai, 2021) and others that can be converted into AC. Last, but not least, reuse and recycle of the biomass waste through the conversion to AC can be an efficient method of agro-industrial waste management (Kongsune et al., 2021). In this study, waste from date palm (leaf sheath date palm fibers) was used to produce AC (LSDPFAC) and its efficiency for adsorbing Pb^{2+} from aqueous solution was evaluated. The date palm (*Phoenix dactylifera L.*) is a tree that belongs to the family of *Arecaceae* and is largely cultivated in the Middle Eastern and North African countries (Al Harthi et al., 2015, Alotaibi et al., 2023). Beside production of edible fruits, the date palm tree produces large amounts of agricultural wastes; for instance one date palm tree can produce up to 40 kg of waste per year, ranging from dried leaves, sheaths, spathes and petioles (Rambabu et al., 2021). Conversion of leaf sheath date palm fibers to AC was effective for removing dye from aqueous solution (Alharbi et al., 2022b), and its efficiency for adsorbing heavy metal deserves further investigation. Utilization of leaf sheath date palm fibers for producing AC can be a good approach to reduce the amount of generated date palm waste in addition to saving the environment by adsorbing Pb^{2+} pollutant from aqueous solution. Therefore, the objective of the current study was to produce AC from leaf sheath date palm fibers as a low-cost precursor via activation with K_2CO_3 under microwave heating for Pb^{2+} adsorption from aqueous solution.

2. Materials and Methods

2.1. Materials

The precursor of leaf sheath date palm fibers was acquired from a private farm near Riyadh city, Saudi Arabia. Potassium carbonate, K_2CO_3 that was used as chemical activating agent was purchased from Sigma Aldrich (St. Louis), while 0.10 M hydrochloric acid, HCl was bought from R&M Chemicals. Synthetic wastewater was prepared by using lead nitrate, $Pb(NO_3)_2$ (assay > 99.0), which was purchased from Sigma Aldrich. Nitrogen gas, N_2 (purity of 99.9%) was supplied by MOX Gases Berhad.

2.2. Preparation of activated carbon (LSDPFAC) from leaf sheath fibers from date palm

Once obtained, the precursor of fibers of leaf sheath from date palm were first dried in open air, chopped into small pieces and finely ground to reach a particle size of 1-2 mm. These materials were transferred to the lab, cleaned with water and placed in an oven at 110°C for 48 hours to dry. The dried precursor was saturated with K_2CO_3 at a ratio of 1:3. The impregnated sample was once again

Preprints (www.preprints.org) | NOT PEER-REVIEWED | Posted: 6 September 2023 doi:10.20944/preprints202309.0321.v1

stored in an oven at 50°C for 24 hours. At this point the material was heated using modified microwave oven (EMW2001W, Sweden) at a radiation power of 616 Watt for 10 minutes. An anoxic atmosphere was created by passing N_2 gas through the container of the sample at 80 cm^3/minutes. After heating was complete the sample, which at that point had been transformed to LSDPFAC, was cooled. The LSDPFAC was soaked in 0.10 M HCl for 30 minutes then rinsed with warm water until the washing solution pH becomes 6-7. Wet LSDPFAC was heated in the oven at 110°C for 24 hours. Once dried, the LSDPFAC was kept inside air-tight container until use for adsorption studies and characterization tests.

2.3. Characterization methods

LSDPFAC was characterised for various parameters. Surface area estimated by use of the Brunauer–Emmett–Teller (BET) and Langmuir function, and pore characteristics, including total pore volume and average pore size, of the LSDPFAC were determined by volumetric adsorption analyser (Micromeritics ASAP 2020). Surface morphology was examined by use of scanning electron microscope (SEM) (Model: LEO SUPRA 55VP, Germany). Analysis of elemental composition was achieved by use of simultaneous thermal analyser (STA) (Model: Model Perkin Elmer STA 6000, USA) and proximate analysis was carried out by thermogravimetric analyser (TGA). Surface chemistry analysis were done by using Fourier transform infrared, FTIR spectroscope (Model: IR Prestige 21 Shimadzu, Japan). The distribution of zeta potential was acquired by employing zeta potential analyser (Model: Zetasizer Nano Series DKSH).

2.4. Equilibrium Study

Several parameters were altered to investigate their effect on uptake of PB^{2+} uptakes and percentage removal from solution. The first parameter investigated was the effect of initial concentration of Pb^{2+}. Six Pb^{2+} solutions with initial concentration from 1.0 to 10 mg/L were prepared inside 6 conical flasks. The volume of each of these solutions was 200 mL. All of these conical flasks were placed into a water bath shaker. Next, accurately weighted 0.2 g of LSDPFAC was added to each conical flask and the mouth sealed with film to prevent evaporation. The temperature of water bath shaker was 30°C and the shaking speed 60 rpm. Every 30 minutes, samples of Pb^{2+} solutions were withdrawn using a syringe and its concentration determined by use of UV-Vis spectrophotometry (Model: Agilent Cary 60, USA). This process was continued until steady state was achieved. The second parameter investigated was temperature. Adsorption was tested at 30, 40 and 50°C, at constant pH. The pH of the Pb^{2+} solution was adjusted to 3, 5, 7, 9, 11 or 13 by use of HCl or NaOH, with temperature fixed at 30°C. Other experimental conditions were fixed as follows: (i) volume solution of 200 mL, (ii) adsorbent weight of 0.2 g and (iii) shaking speed of 60 rpm. Capacity of LSDPFAC to absorb Pb^{2+} and the percentage removal of Pb^{2+} by LSDPFAC were determined (Equations 1 and 2).

$$q_e = \frac{(C_o - C_e)V}{M} \quad (1)$$

$$Removal\ (\%) = \frac{(C_o - C_e)}{C_o} \times 100\% \quad (2)$$

where q_e refers to the amount of Pb^{2+} ions adsorbed by LSDPFAC at equilibrium state (mg/g), C_o and C_e refer to the Pb^{2+} concentration at initial state (mg/L) and equilibrium state (mg/L) respectively, V refers to the volume of Pb^{2+} solution and M refers to the weight of LSDPFAC (g).

2.5. Isotherm study

Knowledges about the connection between adsorbate concentration in the bulk phase and the adsorbate concentration in the solid phase can be determined by studying isotherm models. Hence,

Preprints (www.preprints.org) | NOT PEER-REVIEWED | Posted: 6 September 2023 doi:10.20944/preprints202309.0321.v1

the two most popular isotherm models of Langmuir (Langmuir, 1918) (Equation 3) and Freundlich (Freundlich, 1906) (Equation 4) were used to describe the isotherms.

$$q_e = \frac{Q_m K_L C_e}{1 + K_L C_e} \tag{3}$$

$$q_e = K_F C_e^{1/n_F} \tag{4}$$

where Q_m refers to the Langmuir maximum monolayer adsorption capacity (mg/g), K_L refers to a parameter that has relation with the energy of adsorption (L/mg), K_F refers to the constant of adsorption process (mg/g)(L/mg)$^{1/n}$, n_F refers to the heterogeneity parameter, R refers to the universal gas constant with a fixed value of 8.314 J/mol. K and T is the temperature of the adsorbate solution (K). To fit the non-linear equations of the isotherm models, Microsoft Excel Solver v. 2016 was used. The model that best fitted the adsorption data was chosen based on the correlation coefficient, R^2 as well as root mean squared error (RMSE). The value of RMSE was calculated (Equation 5) (Marrakchi et al., 2020):

$$RMSE = \sqrt{\frac{1}{n-1}\sum_{n=1}^{n}\left(q_{e,exp,n} - q_{e,cal,n}\right)^2} \tag{5}$$

2.6. Kinetic study

The same procedure as that used for the equilibrium study was performed, except that in the kinetic study, concentrations of Pb^{2+} were determined at a pre-determined time between 0 to 180 minutes. The two most popular kinetic models of pseudo-first order (PFO) (Lagergren, 1898) (Equation 6) and pseudo-second order (PSO) PSO (Ho and McKay, 1998) (Equation 7) were both applied.

$$q_t = q_e[1 - exp(-k_1 t)] \tag{6}$$

$$q_t = \frac{k_2 q_e^2 t}{1 + k_2 q_e t} \tag{7}$$

where k_1 and k_2 refer to the rate constant obtained from PFO model (1/min) and rate constant obtained from PSO model (g/mg min) respectively. The kinetic model that best described the adsorption data were judged based on R^2 along with RMSE values.

2.7. Thermodynamic study

Solution temperature influences adsorbate-adsorbent interactivity during the adsorption process. Hence, these effects can be fully understood by conducting a thermodynamic study. There are 4 important thermodynamic parameters: change of enthalpy, △H°, change of entropy, △S°, Gibbs free energy, △G° and Arrhenius activation energy, E_a. To determine the values of ΔH° (kJ/mol) and ΔS° (kJ/mol.K). The relationships among these parameters were described by the Van't Hoff equation (Equation 8).

$$ln\, K_c = \frac{\Delta S°}{R} - \frac{\Delta H°}{RT} \tag{8}$$

where R denotes the universal gas constant with a fixed value of 8.314 J/mol.K, T refers to the solution temperature (K) and K_c is a dimensionless parameter that is recognized as equilibrium constant. K_c can be computed (Lima et al., 2019) (Equation 9).

 doi:10.20944/preprints202309.0321.v1

$$K_c = \frac{1000\frac{mg}{g} \times K_L \times molecular\ weight\ of\ adsorbate \times [adsorbate]^{\circ}}{\gamma} \quad (9)$$

where [adsorbate] is the adsorbate standard concentration where the value of this parameter can be presumed as 1 mol/L at a standard condition, γ is a dimensionless parameter that refers to the activity coefficient for the studied adsorbate and KL is the adsorption constant obtained from Langmuir isotherm model (L/mg). On the other hand, the following formulas as shown below was utilized to find the other two parameters of thermodynamic namely ΔG° (kJ/mol) (Equation 10) and E_a (kJ/mol) (Equation 11), respectively.

$$\Delta G^{\circ} = \triangle H^{\circ} - T\triangle S^{\circ} \quad (10)$$

$$ln\ k_2 = ln\ A - \frac{E_a}{RT} \quad (11)$$

where k_2 refers to the rate constant obtained from PSO kinetic model (g/mg.min) whilst A represents the factor of Arrhenius.

3. Results and discussion

3.1. Characteristics of samples

LSDPFAC had a BET surface area of 560.20 m^2/g and Langmuir surface area of 744.31 m^2/g. This value of BET surface area is similar to that of AC derived from acacia wood-based (AWAC) with a BET of 1045.56 m^2/g (Yusop et al., 2021b). This is because unlike AWAC, LSDPFAC was synthesized with chemical treatment, without undergoing an initial carbonization. Carbonization is known to aid in formation of a network of pores during initial stages of formation of AC. Nonetheless, the decision to omit carbonization stage in producing LSDPFAC was justified by the fact that the process of producing LSDPFAC was simpler and required one less step, and was deemed to be more environmentally friendly, due to the usage of N_2 gas instead of CO_2 gas during microwave heating treatment. The mean BET surface area for LSDPFAC was also contributed by the relatively moderate radiation power (616 Watt) employed in this study. In comparison, a previous study (Hijab et al. (2021) succeeded in producing AC with relatively larger surface area of 1123 m^2/g from date stones by use of radiation power of 850 W. Creation of surface area in LSDPFAC was initially contributed by the chemical agent (K_2CO_3) that penetrated the external layer of precursor to create a network of pores. During microwave activation, K_2CO_3 enhanced degradation of polar components, such as cellulose and lignin in the date palm material (Canales-Flores and Prieto-García, 2020). Total pore volume of LSDPFAC was 0.29 cm^3/g, while mean diameter of pores was 2.47 nm. Since this value is between 2 to 50 nm, pores in LSDPFAC were verified to be mesopores type. Despite using a moderate radiation power of 616 Watt and omission of carbonization, LSDPFAC still contained mesopores, which validated use of K_2CO_3.

The precursor used in this study was confirmed to be appropriate because it had a carbon content of 33.45% and relatively large proportion of fixed carbon of 19.92% (Table 1). In comparison, the fixed carbon in other biomass materials were 18.82% for durian shell (Liu et al., 2021a), 17.10% for almond shell (Martinez et al., 2019), 14.06% for karanja fruit hull (Tan et al., 2019) and 18.12% for coffee husk (Martinez et al., 2019). Chemical activation by K_2CO_3 coupled with microwave heating effectively removed moisture and volatile components from date palm materials. In LSDPFAC, the proportion of elemental carbon increased to 55.67 and fixed carbon increased significantly to 76.52%. Conversely, proximate analysis showed that volatile matter decreased from 66.27 to 5.99%. During microwave heating, moisture and other polar components inside the sample absorb the microwave energy and vibrated at more rapidly, which caused heat to be dissipated. Heat was then causing the volatile matter to evaporate and leave the sample. Moisture increase from 11.92 to 14.26% after chemical treatment and microwave heating. This increment occurred in terms of percentage only and

Preprints (www.preprints.org) | NOT PEER-REVIEWED | Posted: 6 September 2023 doi:10.20944/preprints202309.0321.v1

did not reflect an actual increase in the absolute amount of moisture. Moisture came from addition of deionized water to mix the sample and K_2CO_3 during the chemical activation stage.

Table 1. Elemental and proximate analysis of samples.

Samples	Elemental analysis					Proximate analysis			
	C	H	N	S	Others	Moisture	Volatile matter	Fixed carbon	Ash
Precursor	33.45	3.85	0.97	0.37	61.36	11.92	66.27	19.92	1.90
LSDPFAC	55.67	5.44	0.74	0.37	37.78	14.26	5.99	76.52	3.23

At a magnification of 5000X in SEM images of precursor materials and LSDPFAC, the surface of precursor was seen to be rough, dense and contains no pores Magnification level for SEM images for precursor and LSDPFAC were 5000x (Fig. 1). Pores in LSDPFAC were once occupied by the typical components of lignocellulosic materials such as cellulose, hemicellulose and lignin (Neme et al., 2022), which were subsequently removed, which resulted in formation of the network of pores in LSDPFAC.

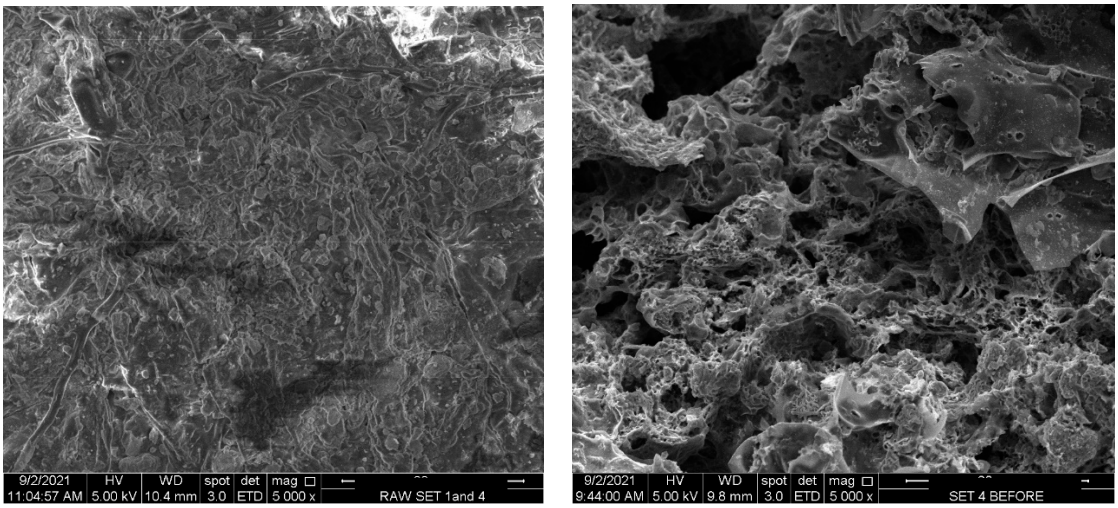

(a) (b)

Figure 1. SEM images of (a) precursor material and (b) LSDLFAC (5000x magnification).

The surface of AC, carried a net charge, which is a function of precursor used, and activation steps applied during synthesis AC. Since adsorption is a surface phenomenon, CV can influence adsorption. This net charge can be verified from distribution of zeta potential (Maršálek and Švidrnoch, 2020) (Figure 2a). The zeta potential for LSDPFAC was -25.5 mV, which indicated that LSDPFAC carried a net negative charge on its surface. AC generally carries a net zeta potential, which is more efficient for adsorbing positive charge (Yusop et al., 2021b).

Preprints (www.preprints.org) | NOT PEER-REVIEWED | Posted: 6 September 2023 doi:10.20944/preprints202309.0321.v1

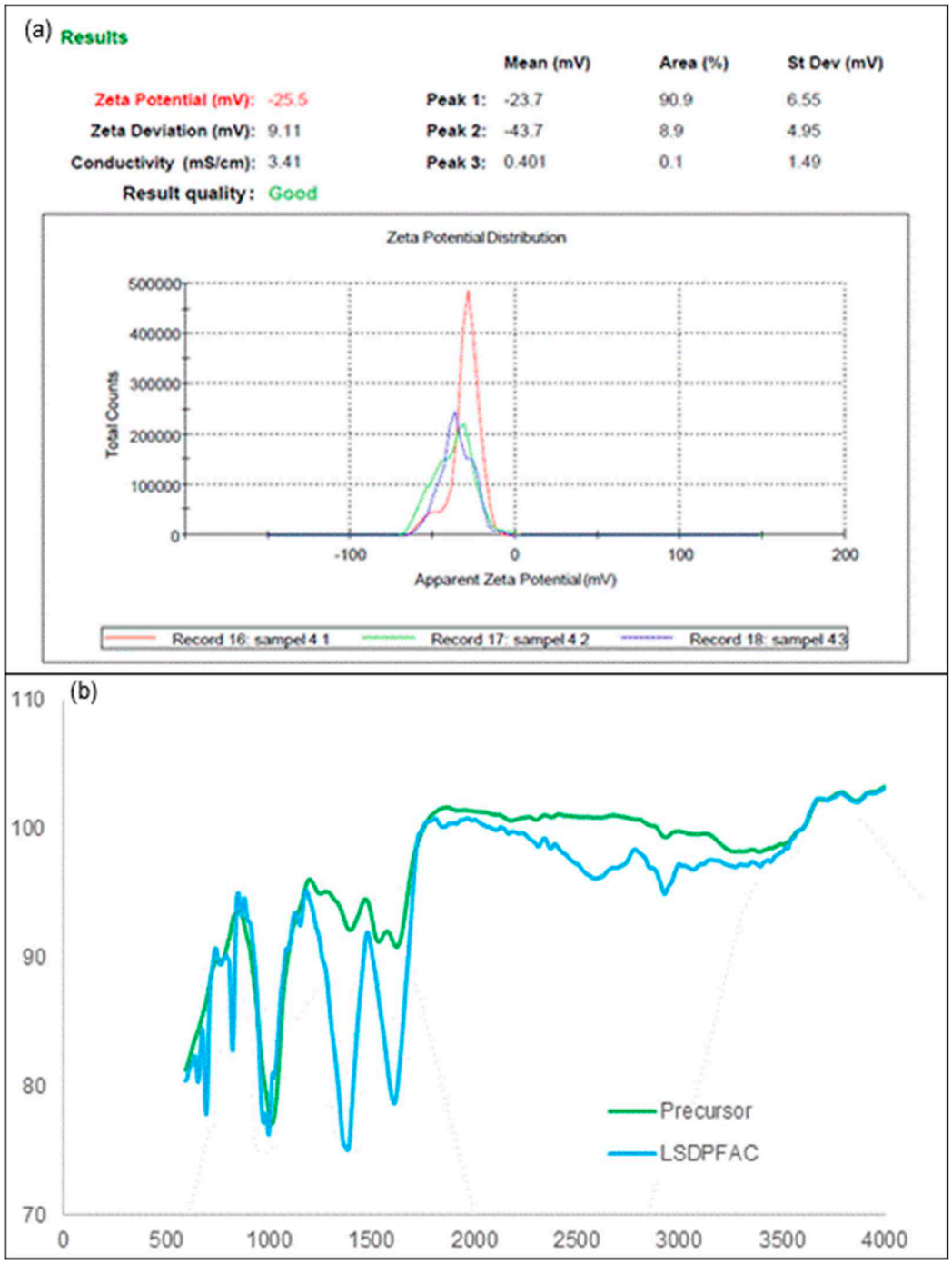

Figure 2. Zeta potential for LSDPFAC (a) and FTIR spectra for precursor materials and LSDPFAC (b).

The surface of precursor material was filled with functional groups of methylene $(CH_2)_n$ as determined by the presence of an FTIR peak of 748 cm^{-1}, which is indicative of aromatic ring stretch C=C-C at a peak of 1583 cm^{-1}, methyl C-H asymmetric stretch at 2970 cm^{-1} and nonbonded hydroxy group OH stretch at 3645 cm^{-1}. (Figure 2b and Table 2) These functional groups did not appear in the surface of LSDPFAC, were removed during activation steps. Some functional groups survived the activation steps, thus appearing in both surfaces of precursor and LSDPFAC. These functional groups were peroxide C-O-O- stretch, which appeared at 860 cm^{-1} in precursor and at 856 and 881 cm^{-1} in LSDPFAC, together with phenol which appeared at 1199 and 1198 cm^{-1} in precursor and LSDPFAC, respectively. Some new peaks, such as tertiary alcohol C-O stretch at 1148 cm^{-1} and carbonate ions at

Preprints (www.preprints.org) | NOT PEER-REVIEWED | Posted: 6 September 2023 doi:10.20944/preprints202309.0321.v1

1477 cm^{-1} were observed on LSDPFAC. Carbonate ions came from the K_2CO_3 utilized during chemical activation.

Table 2. Diagnostic peaks in FTIR spectra of precursor materials and PFAC.

Precursor		LSDPFAC	
Peak (cm^{-1})	**Functional groups**	**Peak (cm^{-1})**	**Functional groups**
748	Methylene –(CH2)n	648	Alkyne C-H bend
860	Peroxides, C-O-O- stretch	677	Alkyne C-H bend
1199	Phenol, C-O stretch	856	Peroxides, C-O-O- stretch
1583	C=C-C Aromatic ring stretch	881	Peroxides, C-O-O- stretch
2970	Methyl C-H asymmetric stretch	1148	Tertiary alcohol, C-O stretch
3645	Nonbonded hydroxy group, OH stretch	1198	Phenol, C-O stretch
		1477	Carbonate ions

3.2. Adsorption equilibrium

To understand effect of duration of contact and initial concentration on adsorption of Pb^{2+}, adsorption as a function of time and plots of percent Pb^{2+} removed as a function of contact time were examined for various initial concentrations of Pb^{2+} (Figure 3a and b). When Pb^{2+} initial concentration was raised from 1 to 10 mg/L, Pb^{2+} adsorption uptakes increased from 0.97 to 8.76 mg/g whilst Pb^{2+} percentage removal decreased from 96.70 to 87.60%. At higher Pb^{2+} initial concentration, more Pb^{2+} ions were available to be adsorbed by LSDPFAC, thus indicated greater adsorption of Pb^{2+} when initial concentrations of Pb^{2+} were greater.

Preprints (www.preprints.org) | NOT PEER-REVIEWED | Posted: 6 September 2023 doi:10.20944/preprints202309.0321.v1

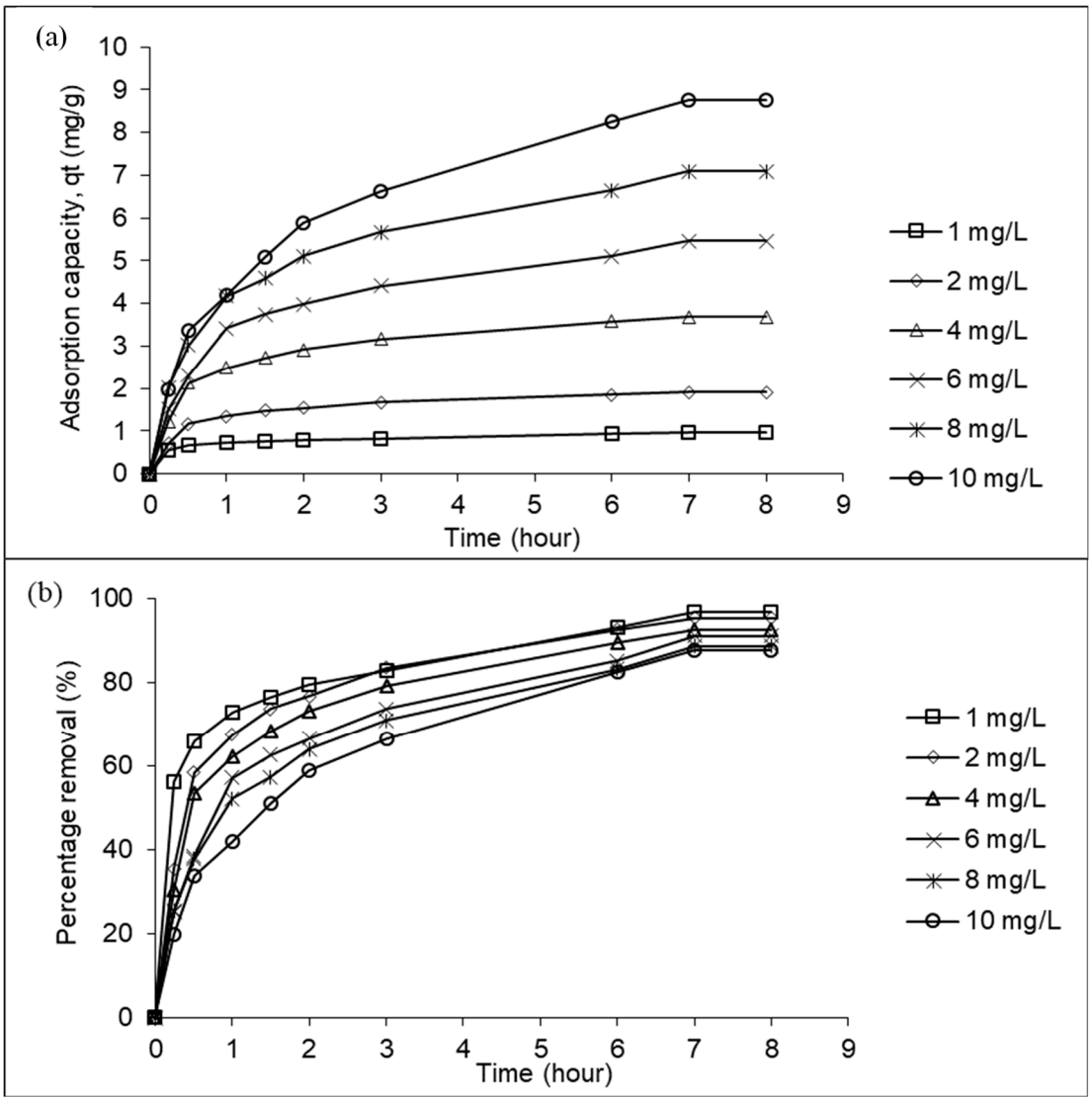

Figure 3. Adsorption of Pb^{2+} by LSDPFAC versus time at 30°C for different initial concentration (a) and percentage removal of Pb^{2+} by LSDPFAC versus time at 30°C for different initial concentration (b).

Adsorption of Pb^{2+} by LSDPFAC was best in alkaline conditions; the greatest amount of Pb^{2+} removed, was 9.15 mg/g, dm at pH 13, while the least, which was 4.51 mg/g was removed at pH 3 of, (Figure 4a). Under acidic conditions of pH 3, existence of more H^+ ions resulted in the surface of LSDPFAC having a net positive charge, hence repulsing the positively charged Pb^{2+} ions. At pH 5, there was an induction effect had reduced a bit in intensity, thus resulting in greater adsorption of Pb^{2+} 4.85 mg/g. At pH 7, amount of H^+ and OH^- were equal, therefore the induction effect on the LSDPFAC was cancel out. Due to effects of surface charge adsorption of Pb^{2+} was greater under alkaline conditions. At pH 11, large amounts of OH^- were available in solution, which created an intense induction on surfaces of LSDPFAC. Adsorption of Pb^{2+} was 9.08 mg/g. At pH 13, adsorption of Pb^{2+} increased only slightly to 9.15 mg/g because increasing the number of OH^- in solution could no longer enhance adsorption.

Preprints (www.preprints.org) | NOT PEER-REVIEWED | Posted: 6 September 2023 doi:10.20944/preprints202309.0321.v1

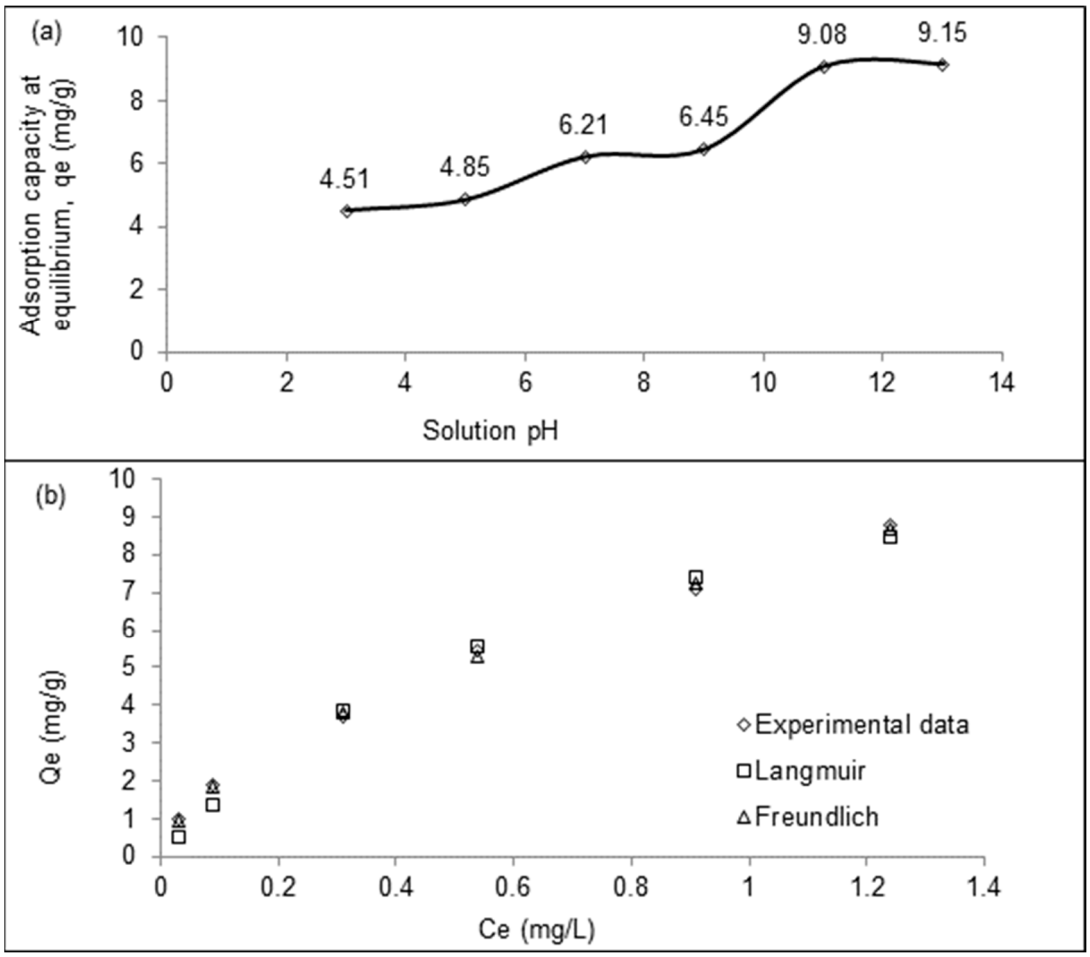

Figure 4. Plots of Pb^{2+} adsorption uptakes by LSDPFAC versus solution pH at 30°C (10 mg/L initial concentration, 0.2 g adsorbent dosage and 200 ml of solution) (a) and plots of isotherm models for Pb^{2+}-LSDLFAC adsorption system at 30°C (b).

3.3. Adsorption isotherm

Adsorption of Pb^{2+} by LSDPFAC could best be described by the Freundlich model (R^2 = 0.9972; RMSE = 0.11 (Table 3; Figure 4b). Thus, Pb^{2+} ions formed a multilayer coverage on the surface of LSDPFAC. The maximum monolayer adsorption capacity, Q_m was 14.10 mg/g, which is comparable to other findings, such as adsorption of Pb^{2+} by leaf extract ZnO nanoparticles, which was 16.26 mg/g (Joshi et al., 2022) and rice husk biochar, which was 22 mg/g (Liu et al., 2021b). Since the heterogeneity factor, n for adsorption of PB^{2+} by LSDPFAC, which was 1.69 was between 1.0 and 10, adsorption of PB^{2+} was favorable (Yusop et al., 2021b).

Table 3. Isotherm parameters for Pb^{2+}-LSDLFAC adsorption system at 30°C.

Isotherm.	Parameters	30 °C
Langmuir	Q_m	14.10
	K_L	1.21
	R^2	0.9976
	RMSE	0.35
Freundlich	K	7.65
	n	1.69
	R^2	0.9972
	RMSE	0.11

3.4. Adsorption kinetics

Preprints (www.preprints.org) | NOT PEER-REVIEWED | Posted: 6 September 2023 doi:10.20944/preprints202309.0321.v1

Kinetics of adsorption Pb^{2+} onto LSDPFAC was best described by PSO (Figures 5a and b). The R^2 values for PSO was greater (average: 0.9967) than that of PFO (average R^2 0.9495) (Table S1). The RMSE value, for PSO of 0.22 was less than that of PFO, which was 1.48. Adsorption of Pb^{2+} by AC produced from cigarette waste (Manfrin et al., 2021) and by AC derived from mangosteen peel (Kongsune et al., 2021) were also best described by PSO model. A consistent decreasing trend was observed in k_2 values (from 0.1168 to 0.0023 g mg^{-1} min^{-1}) as Pb^{2+} initial concentration increased from 1 to 10 mg/L. At greater initial concentration of Pb^{2+}, existence of many Pb^{2+} ions in solution creates a great competition for adsorption process to occur.

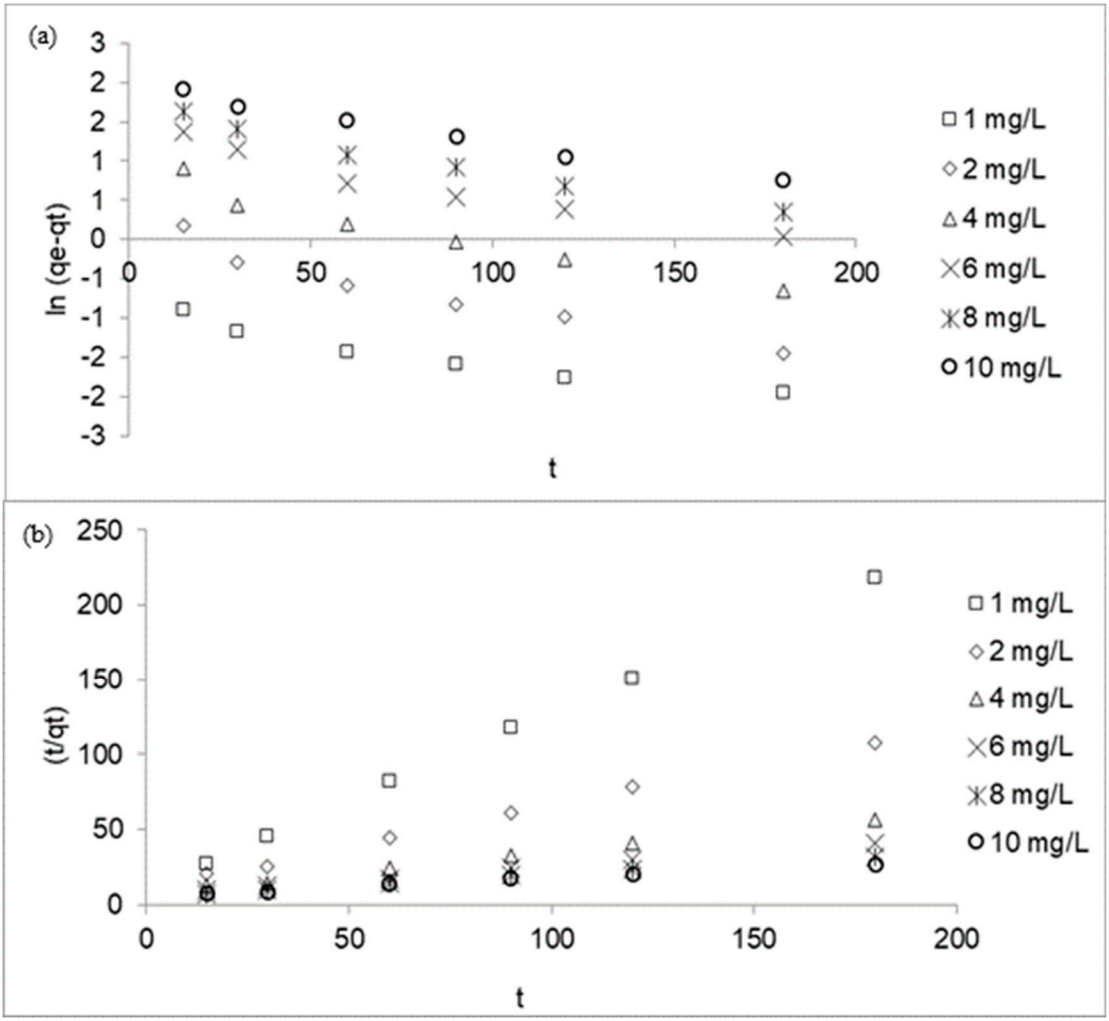

Figure 5. Plots of pseudo-first order kinetic model for Pb^{2+}-LSDLFAC adsorption system at 30°C (a) and plots of pseudo-second order kinetic model for Pb^{2+}-LSDLFAC adsorption system at 30° C (b).

3.5. Adsorption thermodynamic

The thermodynamic nature of adsorption process can be understood by conducting the adsorption process at various temperatures (Figure 6) (Table S2). For instance, when the solution temperature increased from 30 to 50°C, adsorption of Pb^{2+} increased from 8.76 to 8.98 mg/g, which indicated an endothermic adsorption of Pb^{2+} by LSDPFAC (Figure 6), which was consistent with the positive value of $\triangle H°$ of 6.39 kJ/mol. Similarly, adsorption of Cu^{2+}, Pb^{2+}, Cd^{2+} and Zn^{2+} ions by AC-supported silver-silica nanocomposite were all endothermic (Nyirenda et al., 2022). The positive $\triangle S°$ of 0.12 kJ/mol K indicated an increment of randomness at the liquid-solid interface. The value of E_a, which was 15.90 kJ/mol was less than 40 kJ/mol, suggested that adsorption of Pb^{2+} by LSDPFAC was physically governed (Preeti et al., 2021). The negative $\triangle G°$ of -31.28, -32.53 and -33.77 kJ/mol at

Preprints (www.preprints.org) | NOT PEER-REVIEWED | Posted: 6 September 2023 doi:10.20944/preprints202309.0321.v1

temperatures of 303.15, 313.15 and 323.15 K, respectively indicates that adsorption of Pb^{2+} onto LSDPFAC occurred in a spontaneous manner at all temperatures.

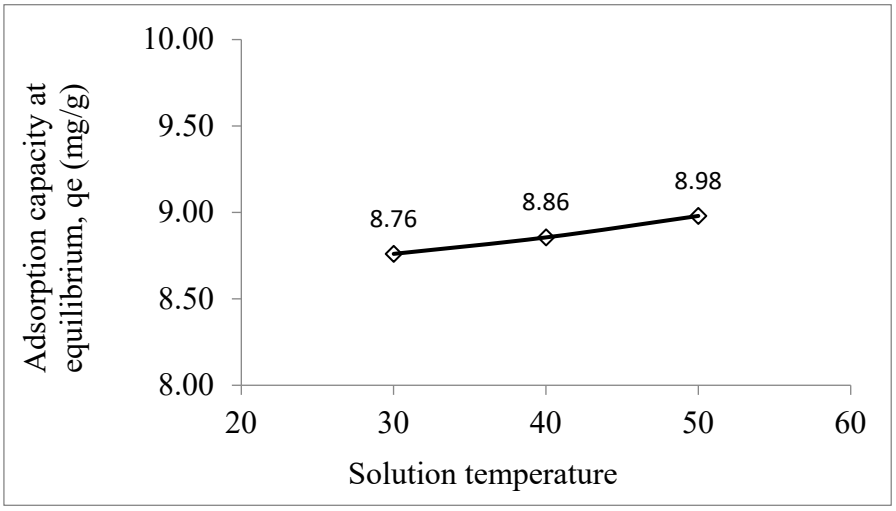

Figure 6. Adsorption capacity of Pb^{2+} onto LSDPFAC versus different solution temperature.

4. Conclusions

Date palm leaf sheath fiber was successfully converted to AC (LSDPFAC) then used to remove Pb^{2+} ions from aqueous solution. The LSDPFAC had BET and Langmuir surface areas, with total pore volume and average pore diameter of 560.20 m^2/g, 744.31 m^2/g, 0.29 cm^3/g and 2.47 nm, respectively. FTIR spectrum revealed that LSDPFAC's surface were occupied by alkyne C-H bend, peroxides C-O-O stretch, tertiary alcohol C-O stretch, and phenol C-O stretch. When Pb^{2+} initial concentration increased from 1 to 10 mg/L, Pb^{2+} adsorption uptakes increased from 0.97 to 8.76 mg/g whilst Pb^{2+} percentage removal decreased from 96.70 to 87.60%. The greatest rate of adsorption of Pb^{2+} was 9.15 mg/g at pH 13 and 8.98 mg/g at temperature of 50°C. Adsorption could be well described by the Freundlich and PSO models, respectively. Langmuir monolayer adsorption capacity, Q_m was found to be 14.10 mg/g. The results of the thermo-dynamic study revealed that the adsorption process was endothermic, spontaneous and governed by physisorption. The findings of this study demonstrate that date palm leaf sheath fiber can be used as a low-cost precursor of activated carbon that showed a promising potential for application in Pb^{2+} removal from contaminated water.

Author Contributions: For research articles with several authors, a short paragraph specifying their individual contributions must be provided. The following statements should be used "Conceptualization, X.X. and Y.Y.; methodology, X.X.; software, X.X.; validation, X.X., Y.Y. and Z.Z.; formal analysis, X.X.; investigation, X.X.; resources, X.X.; data curation, X.X.; writing—original draft preparation, X.X.; writing—review and editing, X.X.; visualization, X.X.; supervision, X.X.; project administration, X.X.; funding acquisition, Y.Y. All authors have read and agreed to the published version of the manuscript." Please turn to the CRediT taxonomy for the term explanation. Authorship must be limited to those who have contributed substantially to the work reported.

Funding: Please add: "This research received no external funding" or "This research was funded by NAME OF FUNDER, grant number XXX" and "The APC was funded by XXX". Check carefully that the details given are accurate and use the standard spelling of funding agency names at https://search.crossref.org/funding. Any errors may affect your future funding.

Data Availability Statement: In this section, please provide details regarding where data supporting reported results can be found, including links to publicly archived datasets analyzed or generated during the study. Please refer to suggested Data Availability Statements in section "MDPI Research Data Policies" at https://www.mdpi.com/ethics. You might choose to exclude this statement if the study did not report any data.

Acknowledgments: This research project was funded by Researchers Supporting Project number (RSPD2023R633), king Saud University, Riyadh, Saudi Arabia.

Conflicts of Interest: Declare conflicts of interest or state "The authors declare no conflict of interest." Authors must identify and declare any personal circumstances or interest that may be perceived as inappropriately

influencing the representation or interpretation of reported research results. Any role of the funders in the design of the study; in the collection, analyses or interpretation of data; in the writing of the manuscript, or in the decision to publish the results must be declared in this section. If there is no role, please state "The funders had no role in the design of the study; in the collection, analyses, or interpretation of data; in the writing of the manuscript, or in the decision to publish the results".

References

1. AFROZE, S. & SEN, T. K. 2018. A Review on Heavy Metal Ions and Dye Adsorption from Water by Agricultural Solid Waste Adsorbents. *Water, Air, and Soil Pollution,* 229.
2. AL HARTHI, S., MAVAZHE, A., AL MAHROQI, H. & KHAN, S. A. 2015. Quantification of phenolic compounds, evaluation of physicochemical properties and antioxidant activity of four date (Phoenix dactylifera L.) varieties of Oman. *Journal of Taibah University Medical Sciences,* 10**,** 346-352.
3. ALHARBI, H. A., HAMEED, B. H., ALOTAIBI, K. D., AL-OUD, S. S. & AL-MODAIHSH, A. S. 2022a. Recent methods in the production of activated carbon from date palm residues for the adsorption of textile dyes: A review.
4. ALHARBI, H. A., HAMEED, B. H., ALOTAIBI, K. D., ALOUD, S. S. & AL-MODAIHSH, A. S. 2022b. Mesoporous Activated Carbon from Leaf Sheath Date Palm Fibers by Microwave-Assisted Phosphoric Acid Activation for Efficient Dye Adsorption. *ACS omega*.
5. ALOTAIBI, K. D., ALHARBI, H. A., YAISH, M. W., AHMED, I., ALHARBI, S. A., ALOTAIBI, F. & KUZYAKOV, Y. 2023. Date palm cultivation: A review of soil and environmental conditions and future challenges. *Land Degradation & Development*.
6. AZAMAT, J., SARDROODI, J. J., POURSOLTANI, L. & JAHANSHAHI, D. 2021. Functionalized boron nitride nanosheet as a membrane for removal of Pb2+ and Cd2+ ions from aqueous solution. *Journal of Molecular Liquids,* 321**,** 114920.
7. AZIZ, A., KHAN, M. N. N., YUSOP, M. F. M., JAYA, M. J. J., JAYA, M. A. T. & AHMAD, M. A. 2021. Single-Stage Microwave-Assisted Coconut-Shell-Based Activated Carbon for Removal of Dichlorodiphenyltrichloroethane (DDT) from Aqueous Solution: Optimization and Batch Studies. *International Journal of Chemical Engineering,* 2021.
8. AZMIER, M., ASWAREUSOFF, M., OLADOYE, P., ADEGOKE, K. A. & BELL, O. 2021. Optimization and batch studies on adsorption of Methylene blue dye using pomegranate fruit peel based adsorbent. *Chemical Data Collections,* 32**,** 100676.
9. CANALES-FLORES, R. A. & PRIETO-GARCÍA, F. 2020. Taguchi optimization for production of activated carbon from phosphoric acid impregnated agricultural waste by microwave heating for the removal of methylene blue. *Diamond and Related Materials,* 109**,** 108027.
10. DU, J., ZHOU, A., LIN, X. & BU, Y. 2022. Adsorption mechanism of Pb2+ in montmorillonite nanopore under various temperatures and concentrations. *Environmental Research,* 209**,** 112817.
11. FIRDAUS, M. Y. M., AZIZ, A. & AZMIER AHMAD, M. 2022. Conversion of teak wood waste into microwave-irradiated activated carbon for cationic methylene blue dye removal: Optimization and batch studies. *Arabian Journal of Chemistry,* 15**,** 104081.
12. FREUNDLICH, H. M. F. 1906. Over the adsorption in solution. *The Journal of Physical Chemistry* 57**,** 385-471.
13. GHERASIM, C. V., KŘIVČÍK, J. & MIKULÁŠEK, P. 2014. Investigation of batch electrodialysis process for removal of lead ions from aqueous solutions. *Chemical Engineering Journal,* 256**,** 324-334.
14. GOSWAMI, L., ARUL MANIKANDAN, N., PAKSHIRAJAN, K. & PUGAZHENTHI, G. 2017. Simultaneous heavy metal removal and anthracene biodegradation by the oleaginous bacteria Rhodococcus opacus. *3 Biotech,* 7.
15. GUPTA, K. M., ZHANG, K. & JIANG, J. 2018. Efficient removal of Pb2+ from aqueous solution by an ionic covalent−organic framework: Molecular simulation study. *Industrial and Engineering Chemistry Research,* 57**,** 6477-6482.
16. HAGHBIN, M. R. & NIKNAM SHAHRAK, M. 2021. Process conditions optimization for the fabrication of highly porous activated carbon from date palm bark wastes for removing pollutants from water. *Powder Technology,* 377**,** 890-899.
17. HIJAB, M., PARTHASARATHY, P., MACKEY, H. R., AL-ANSARI, T. & MCKAY, G. 2021. Minimizing adsorbent requirements using multi-stage batch adsorption for malachite green removal using microwave date-stone activated carbons. *Chemical Engineering and Processing - Process Intensification,* 167**,** 108318.
18. HO, Y. S. & MCKAY, G. 1998. Sorption of dye from aqueous solution by peat. *Chemical Engineering Journal,* 70**,** 115-124.
19. IQBAL, M. O. & YAHYA, E. B. 2021. In vivo assessment of reversing aminoglycoside antibiotics nephrotoxicity using Jatropha mollissima crude extract. *Tissue and Cell,* 72**,** 101525.

20. JOSHI, N. C., RAWAT, B. S., KUMAR, P., KUMAR, N., UPADHYAY, S., CHETANA, S., GURURANI, P. & KIMOTHI, S. 2022. Sustainable synthetic approach and applications of ZnO/r-GO in the adsorption of toxic Pb2+ and Cr6+ ions. *Inorganic Chemistry Communications,* 145**,** 110040.
21. KONGSUNE, P., RATTANAPAN, S. & CHANAJAREE, R. 2021. The removal of Pb2+ from aqueous solution using mangosteen peel activated carbon: Isotherm, kinetic, thermodynamic and binding energy calculation. *Groundwater for Sustainable Development,* 12**,** 100524.
22. LAGERGREN, S. K. 1898. About the Theory of So-called Adsorption of Soluble Substances. *Sven. Vetenskapsakad. Handingarl,* 24**,** 1-39.
23. LAI, H. J. 2021. Adsorption of Remazol Brilliant Violet 5R (RBV-5R) and Remazol Brilliant Blue R (RBBR) from Aqueous Solution by Using Agriculture Waste. *Tropical Aquatic and Soil Pollution,* 1**,** 11-23.
24. LANGMUIR, I. 1918. The adsorption of gases on plane surfaces of glass, mica and platinum. *Journal of the American Chemical Society,* 40**,** 1361-1403.
25. LI, S., CHO, M.-K., LEE, K., DENG, S., ZHAO, L., YUAN, X. & WANG, J. 2022. Diamond in the rough: Polishing waste polyethylene terephthalate into activated carbon for CO2 capture. *Science of The Total Environment,* 834**,** 155262.
26. LIMA, E. C., HOSSEINI-BANDEGHARAEI, A., MORENO-PIRAJÁN, J. C. & ANASTOPOULOS, I. 2019. A critical review of the estimation of the thermodynamic parameters on adsorption equilibria. Wrong use of equilibrium constant in the Van't Hoof equation for calculation of thermodynamic parameters of adsorption. *Journal of Molecular Liquids,* 273**,** 425-434.
27. LIU, H., LIU, J., HUANG, H., EVRENDILEK, F., WEN, S. & LI, W. 2021a. Optimizing bioenergy and by-product outputs from durian shell pyrolysis. *Renewable Energy,* 164**,** 407-418.
28. LIU, L., HUANG, Y., CAO, J., HU, H., DONG, L., ZHA, J., SU, Y., RUAN, R. & TAO, S. 2021b. Qualitative and relative distribution of Pb2+ adsorption mechanisms by biochars produced from a fluidized bed pyrolysis system under mild air oxidization conditions. *Journal of Molecular Liquids,* 323**,** 114600.
29. LIU, X., WANG, Y. & CHANG, J. 2021c. A review on the incorporation and potential mechanism of heavy metals on the recovered struvite from wastewater. *Water Research,* 207**,** 117823.
30. LYSTVAN, K., LISTVAN, V., SHCHERBAK, N. & KUCHUK, M. 2021. Rhizoextraction Potential of Convolvulus tricolor Hairy Roots for Cr6+, Ni2+, and Pb2+ Removal from Aqueous Solutions. *Applied Biochemistry and Biotechnology,* 193**,** 1215-1230.
31. MANFRIN, J., GONÇALVES JR, A. C., SCHWANTES, D., CONRADI JR, E., ZIMMERMANN, J. & ZIEMER, G. L. 2021. Development of biochar and activated carbon from cigarettes wastes and their applications in Pb2+ adsorption. *Journal of Environmental Chemical Engineering,* 9**,** 104980.
32. MARRAKCHI, F., HAMEED, B. H. & BOUAZIZ, M. 2020. Mesoporous and high-surface-area activated carbon from defatted olive cake by-products of olive mills for the adsorption kinetics and isotherm of methylene blue and acid blue 29. *Journal of Environmental Chemical Engineering,* 8**,** 104199.
33. MARŠÁLEK, R. & ŠVIDRNOCH, M. 2020. The adsorption of amitriptyline and nortriptyline on activated carbon, diosmectite and titanium dioxide. *Environmental Challenges,* 1**,** 100005.
34. MARTINEZ, C. L. M., ROCHA, E. P. A., CARNEIRO, A. O., GOMES, F. J. B., BATALHA, L. A. R. & VAKKILAINEN, E. 2019. Characterization of residual biomasses from the coffee production chain and assessment the potential for energy purposes. *Biomass & Bioenergy,* 120**,** 68-76.
35. MBARKI, F., SELMI, T., KESRAOUI, A. & SEFFEN, M. 2022. Low-cost activated carbon preparation from Corn stigmata fibers chemically activated using H3PO4, ZnCl2 and KOH: Study of methylene blue adsorption, stochastic isotherm and fractal kinetic. *Industrial Crops and Products,* 178**,** 114546.
36. MIRZABEYGI, M., ABBASNIA, A., YUNESIAN, M., NODEHI, R. N., YOUSEFI, N., HADI, M. & MAHVI, A. H. 2017. Heavy metal contamination and health risk assessment in drinking water of Sistan and Baluchistan, Southeastern Iran. *Human and Ecological Risk Assessment: An International Journal,* 23**,** 1893-1905.
37. NEME, I., GONFA, G. & MASI, C. 2022. Activated carbon from biomass precursors using phosphoric acid: A review. *Heliyon,* 8**,** e11940.
38. NYIRENDA, J., KALABA, G. & MUNYATI, O. 2022. Synthesis and characterization of an activated carbon-supported silver-silica nanocomposite for adsorption of heavy metal ions from water. *Results in Engineering,* 15**,** 100553.
39. PREETI, BANERJEE, S., DEBNATH, A. & SINGH, V. 2021. Gum ghatti-alginate hybrid bead derived titania spheres for deep removal of toxic dye Remazol Brilliant Violet from aqueous solutions. *Environmental Nanotechnology, Monitoring & Management,* 15**,** 100459.
40. QUESADA, H. B., DE ARAÚJO, T. P., CUSIOLI, L. F., DE BARROS, M. A. S. D., GOMES, R. G. & BERGAMASCO, R. 2022. Caffeine removal by chitosan/activated carbon composite beads: Adsorption in tap water and synthetic hospital wastewater. *Chemical Engineering Research and Design,* 184**,** 1-12.

41. RAJENDRAN, S., PRIYA, A. K., SENTHIL KUMAR, P., HOANG, T. K. A., SEKAR, K., CHONG, K. Y., KHOO, K. S., NG, H. S. & SHOW, P. L. 2022. A critical and recent developments on adsorption technique for removal of heavy metals from wastewater-A review. *Chemosphere,* 303**,** 135146.
42. RAMBABU, K., ALYAMMAHI, J., BHARATH, G., THANIGAIVELAN, A., SIVARAJASEKAR, N. & BANAT, F. 2021. Nano-activated carbon derived from date palm coir waste for efficient sequestration of noxious 2,4-dichlorophenoxyacetic acid herbicide. *Chemosphere,* 282.
43. RAMUTSHATSHA-MAKHWEDZHA, D., MAVHUNGU, A., MOROPENG, M. L. & MBAYA, R. 2022. Activated carbon derived from waste orange and lemon peels for the adsorption of methyl orange and methylene blue dyes from wastewater. *Heliyon***,** e09930.
44. REZANIA, S., MOJIRI, A., PARK, J., NAWROT, N., WOJCIECHOWSKA, E., MARRAIKI, N. & ZAGHLOUL, N. S. S. 2022. Removal of lead ions from wastewater using lanthanum sulfide nanoparticle decorated over magnetic graphene oxide. *Environmental Research,* 204.
45. TAN, Y. L., ABDULLAH, A. Z. & HAMEED, B. H. 2019. Product distribution of the thermal and catalytic fast pyrolysis of karanja (Pongamia pinnata) fruit hulls over a reusable silica-alumina catalyst. *Fuel,* 245**,** 89-95.
46. XIANG, H., MIN, X., TANG, C.-J., SILLANPÄÄ, M. & ZHAO, F. 2022. Recent advances in membrane filtration for heavy metal removal from wastewater: A mini review. *Journal of Water Process Engineering,* 49**,** 103023.
47. XU, J., CAO, Z., ZHANG, Y., YUAN, Z., LOU, Z., XU, X. & WANG, X. 2018. A review of functionalized carbon nanotubes and graphene for heavy metal adsorption from water: Preparation, application, and mechanism. *Chemosphere,* 195**,** 351-364.
48. YUSOP, M. F. M., AHMAD, M. A., ROSLI, N. A., GONAWAN, F. N. & ABDULLAH, S. J. 2021a. Scavenging malachite green dye from aqueous solution using durian peel based activated carbon. *Malaysian Journal of Fundamental and Applied Sciences,* 17**,** 95-103.
49. YUSOP, M. F. M., AHMAD, M. A., ROSLI, N. A. & MANAF, M. E. A. 2021b. Adsorption of cationic methylene blue dye using microwave-assisted activated carbon derived from acacia wood: Optimization and batch studies. *Arabian Journal of Chemistry,* 14**,** 103122.
50. YUSOP, M. F. M., JAYA, E. M. J. & AHMAD, M. A. 2022a. Single-stage microwave assisted coconut shell based activated carbon for removal of Zn(II) ions from aqueous solution – Optimization and batch studies. *Arabian Journal of Chemistry,* 15**,** 104011.
51. YUSOP, M. F. M., MOHD JOHAN JAYA, E., MOHD DIN, A. T., BELLO, O. S. & AHMAD, M. A. 2022b. Single-Stage Optimized Microwave-Induced Activated Carbon from Coconut Shell for Cadmium Adsorption. 45**,** 1943-1951.
52. ZENG, G., WAN, J., HUANG, D., HU, L., HUANG, C., CHENG, M., XUE, W., GONG, X., WANG, R. & JIANG, D. 2017. Precipitation, adsorption and rhizosphere effect: The mechanisms for Phosphate-induced Pb immobilization in soils—A review. *Journal of Hazardous Materials,* 339**,** 354-367.
53. ZHANG, X., LIN, Q., LUO, S., RUAN, K. & PENG, K. 2018. Preparation of novel oxidized mesoporous carbon with excellent adsorption performance for removal of malachite green and lead ion. *Applied Surface Science,* 442**,** 322-331.
54.